

A Computational Study of the Complex Dichlorobis(pyrazinamido)platinum(II), [PtCl₂(PZA)₂], Applying a Mixed-Level Factorial Design

Paola Araujo S. Oliveira,^a Lucas M. Sartori,^b Nicolás A. Rey,^b Hélio F. Dos Santos,^a
Marcone Augusto L. De Oliveira^c and Luiz Antônio S. Costa^{*a}

^aNúcleo de Estudos em Química Computacional (NEQC), Departamento de Química, Instituto de Ciências Exatas (ICE), Universidade Federal de Juiz de Fora, 36036-900 Juiz de Fora-MG, Brazil

^bLaboratório de Síntese Orgânica e Química de Coordenação Aplicada a Sistemas Biológicos (LABSO), Departamento de Química, Centro Técnico Científico (CTC), Pontifícia Universidade Católica do Rio de Janeiro, 22453-900 Rio de Janeiro-RJ, Brazil

^cGrupo de Química Analítica e Quimiometria (GQAQ), Departamento de Química, Instituto de Ciências Exatas (ICE), Universidade Federal de Juiz de Fora, 36036-900 Juiz de Fora-MG, Brazil

As pesquisas na área de Química Medicinal têm envolvido diversos aspectos focando o tratamento de doenças tais como câncer, em especial, a combinação de potenciais terapêuticos apresentados por moléculas distintas. Visando isso, realizou-se um estudo computacional combinando a pirazinamida (PZA), um imprescindível tuberculostático com a cisplatina, importante antitumoral, para obter as melhores características de ambas. Foi feita a busca por uma estrutura mais estável para o complexo de estequiometria PZA:platina(II) 2:1 *cis*-[PtCl₂(PZA)₂], ou *cis*-diclorobis(pirazinamido)-platina(II), utilizando para isso a teoria do funcional densidade (DFT) associada ao uso de um planejamento fatorial misto de dois fatores do tipo 5 × 3, para um total de 15 experimentos. Através da avaliação da superfície de resposta e da realização de sete experimentos para validação do modelo, inferiu-se que a estrutura de maior estabilidade refere-se àquela com o diedro 2Cl/1Pt/5O/7C sob um ângulo de 18,9°.

Research in Medicinal Chemistry has involved numerous aspects focusing on the treatment of several kinds of diseases, such as cancer, especially by the combination of therapeutic potentials by using different molecules. With this aim, a computational study combining pyrazinamide (PZA), an indispensable tuberculostatic drug, and cisplatin, an important antitumoral agent, was conducted to combine the best features of both compounds. A search for the most stable structure of the platinum(II)-PZA complex at a 2:1 stoichiometry: diclorodi(pyrazinamido)platinum(II), or *cis*-[PtCl₂(PZA)₂], was performed, using functional theory (DFT) associated to a mixed-level factorial design of two factors type 5 × 3, totaling 15 experiments. After evaluating the response surface and following the performance of seven experiments to validate the area identified as optimal, the most stable structure is that in which the dihedral 2Cl/1Pt/5O/7C is at an 18.9° angle.

Keywords: DFT, platinum(II) complex, pyrazinamide, mixed-level factorial design

Introduction

Platinum complexes have been widely used to treat solid tumors¹⁻² since cisplatin entered the clinical area as an anticancer drug,³⁻⁵ revealing a new era in Bioinorganic Chemistry research. In addition to the platinum(II) complexes, cisplatin, carboplatin and oxaliplatin,⁶ other metalodrugs have appeared in the field and play an important

role in medicinal chemistry.^{7,8} In addition, the ligands coordinated to the platinum atom, even in its isolated form, participate intensively in the clinical treatment of several types of diseases. The metal center, along with the ligands, plays a relevant role in the mechanism of action of diseases such as cancer.⁸⁻¹¹ An important class of ligands is one that includes the isoniazid (INH) and pyrazinamide (PZA) drugs (Figure 1), typically used in tuberculosis (TB) treatments.¹²

TB is a serious illness, spread by air, which can infect all the organs of the body. The infection caused by

*e-mail: luiz.costa@ufjf.edu.br

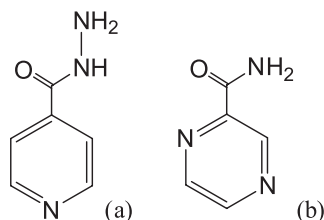


Figure 1. Chemical structures of (a) isoniazid (INH) and (b) pyrazinamide (PZA).

the Koch bacillus begins when the bacillus reaches the pulmonary alveoli, and may then further spread to the lymphatic nodes and other organs until it reaches the brain, bones and kidneys.^{13,14} TB is curable in practically 100% of the new cases, depicting the therapeutical potential of drugs related to this disease.

Even after so many years since the discovery of antibacterial drugs like PZA, their mechanism of action, as well as bacterial resistance to these drugs, is not yet fully revealed. The understanding of such mechanisms is intrinsically related to the structural features of these compounds. Many analytical techniques have aided in this sense, but very few steps have been given regarding computational methods, a loss since theoretical chemistry along the years has provided important data based on new and promising molecules or even those well described.¹⁵⁻¹⁷

Within the last decade, platinum-based anticancer drugs have resurfaced. Besides cisplatin compounds and some of their analogues, which induce apoptosis in tumoral cells via DNA damage, these compounds can react in a non-selective way with a variety of other biomolecules, such as proteins and phospholipids.¹⁸ The possibility of studying a platinum(II) complex in which the ligands are PZA molecules began being explored recently from an experimental point of view by the group coordinated by Professor Nicolás A. Rey at Pontifícia Universidade Católica do Rio de Janeiro (Rio de Janeiro, Brazil), with theoretical support given by our group (NEQC) at Universidade Federal de Juiz de Fora (Minas Gerais, Brazil). This proposal attempts to link the best of two different classes of compounds: the lesser toxic effects of pyrazinamide with the large antitumoral spectrum of activity of platinum complexes, based on the well-established concept of hybrid drugs (see as example the work of Guddneppanavar *et al.*¹⁹).

In the present study, a novel compound, namely *cis*-[PtCl₂(PZA)₂] or *cis*-dichlorobis(pyrazinamido) platinum(II) (Figure 2), was studied by density functional theory (DFT) using a mixed-level factorial design as an auxiliary tool to aid in experimental planning and data interpretation in order to minimize computational

time and effort, and to improve the assessment regarding certain information, such as molecular energies and their relationship to dihedral angles.²⁰

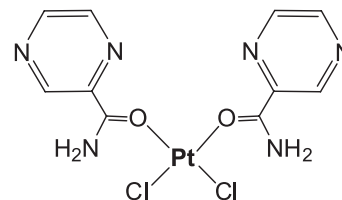


Figure 2. Chemical structure of *cis*-dichlorobis(pyrazinamido) platinum(II) or *cis*-[PtCl₂(PZA)₂].

Methodology

Full unconstrained geometry optimizations were performed using the B3LYP DFT^{21,22} with 6-311+G(2d,p) Pople's polarized split valence basis set for all the compound atoms (C, N, O, H and Cl),^{23,24} except for platinum, for which the relativistic effective core potential LANL2DZ was used.²⁵⁻²⁷ A similar level of theory has been recently applied for cisplatin derivatives, giving satisfactory results for structures and energies.^{28,29} The thermodynamic properties were calculated at 298 K and 1 atm in gas phase within the same level of theory used for geometry optimization. Also, a rigid potential energy surface scan was performed in order to evaluate other possible conformations of *cis*-[PtCl₂(PZA)₂],³⁰ using the same level of theory cited above. All calculations were performed using the Gaussian 09 quantum mechanical package as available at the NEQC-UFJF servers.³¹

A 5 × 3 mixed-level factorial design containing factors at five (−1, −0.5, 0, 0.5 and +1 for the dihedral angle factor) and three (−1, 0, +1 for the dihedral factor) mixed levels was randomly conducted, totaling 15 experiments. These factors are defined as follows and highlighted in Table 1 and Figure 3. The matrix of contrast coefficients, factors, levels and energy responses is shown in Table 2.

In order to clarify which atoms were involved in the statistical analysis, Figure 4 shows the D1, D2 and

Table 1. Relationships between factors, dihedral angles and the dihedral labels

| Factor | Dihedral angle (X ₁) / degree | Dihedral (X ₂) ^a |
|--------|---|---|
| −1 | 0 | D1 |
| −0.5 | 45 | − |
| 0 | 90 | D2 |
| 0.5 | 135 | − |
| 1 | 180 | D3 |

^aX₂: dihedral labels: D1: 4O/6C/11C/12N; D2: 2Cl/1Pt/5O/7C; D3: 1Pt/5O/7C/9C, according to the labels of Figure 3 and 4.

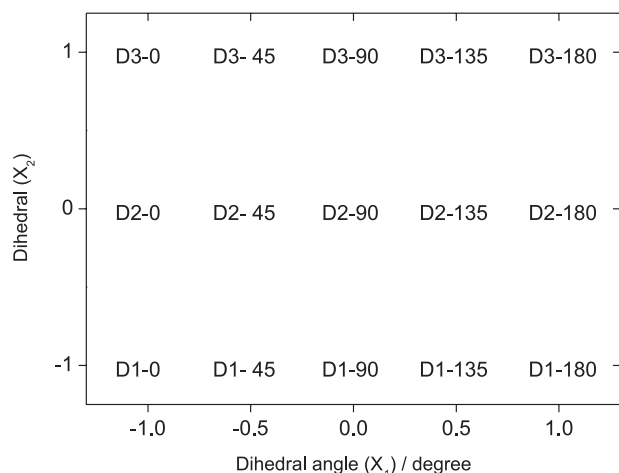


Figure 3. General scheme of the mixed-level factorial design 5×3 used in the present study.

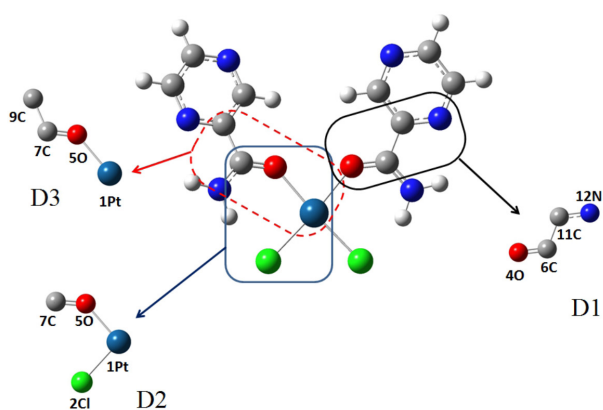


Figure 4. Atom labels of D1: 4O/6C/11C/12N, D2: 2Cl/1Pt/5O/7C and D3: 1Pt/5O/7C/9C.

Table 2. Matrix of contrast coefficients, factors, levels and responses for a 5×3 mixed experimental design

| Response | Mean | X ₁ | X ₂ | X ₁ X ₁ | X ₂ X ₂ | X ₁ X ₂ | Energy / a.u. |
|----------|------|----------------|----------------|-------------------------------|-------------------------------|-------------------------------|---------------|
| 1 | 1 | -1 | -1 | 1 | 1 | 1 | -1904.240515 |
| 2 | 1 | -0.5 | -1 | 0.25 | 1 | 0.5 | -1904.226578 |
| 3 | 1 | 0 | -1 | 0 | 1 | 0 | -1904.257614 |
| 4 | 1 | 0.5 | -1 | 0.25 | 1 | -0.5 | -1904.257613 |
| 5 | 1 | 1 | -1 | 1 | 1 | -1 | -1904.240515 |
| 6 | 1 | -1 | 0 | 1 | 0 | 0 | -1905.655901 |
| 7 | 1 | -0.5 | 0 | 0.25 | 0 | 0 | -1905.658634 |
| 8 | 1 | 0 | 0 | 0 | 0 | 0 | -1905.651833 |
| 9 | 1 | 0.5 | 0 | 0.25 | 0 | 0 | -1905.666190 |
| 10 | 1 | 1 | 0 | 1 | 0 | 0 | -1904.956282 |
| 11 | 1 | -1 | 1 | 1 | 1 | -1 | -1905.659706 |
| 12 | 1 | -0.5 | 1 | 0.25 | 1 | -0.5 | -1905.653522 |
| 13 | 1 | 0 | 1 | 0 | 1 | 0 | -1905.643420 |
| 14 | 1 | 0.5 | 1 | 0.25 | 1 | 0.5 | -1905.372054 |
| 15 | 1 | 1 | 1 | 1 | 1 | 1 | -1905.672048 |

X₁: dihedral angle (degrees): (-1): 0°; (-0.5): 45°; (0): 90°; (0.5): 135°; (+1): 180°. X₂: dihedral (labels): (-1):D1 = 4O/6C/11C/12N; (0):D2 = 2Cl/1Pt/5O/7C; (+1):D3 = 1Pt/5O/7C/9C

D3 dihedral angles detached from the optimized structure of [PtCl₂(PZA)₂] (I). The optimized dihedral angles were D1: -178.7°; D2: 22.1° and D3: 177.5°. Since rigid scan calculations are performed by a single point energy evaluation over a rectangular grid involving selected internal coordinates, it was chosen to perform the variation of these dihedral angles as independents. Our intention was to perform a factorial design test with the minimum factors as possible.

After the experiments, statistical analyses were conducted^{32,33} and the coefficients for determining the statistical model prediction were calculated according to equation 1 after observing the results of each experiment.

$$b = (X'X)^{-1}X'y \quad (1)$$

where vector *b* represents the model parameter estimators and *X* and *y* are the matrix and vector, respectively, according to Table 2.

Factorial design calculations were performed in Microsoft Office® Excel 2007 software. Basic statistical analysis such as normality test (Shapiro-Wilk test) was performed using SPSS 8.0 for Windows. The surface response was plotted using MATLAB environment.

Results and Discussion

Structural analyses

Initially, we began the computational work with two different conformations for the molecule [PtCl₂(PZA)₂]

(Figure 4). In both cases, the *cis* isomer was considered and PZA was coordinated to the platinum center through the oxygen atom. This proposal was experimentally verified by the spectroscopic data acquired by Sartori and Rey; those results were not published so far. The vibrational frequency at 1714 cm^{-1} for the free PZA ligand is attributed to a coupling involving the stretching mode of carbonyl group ν (C=O) associated to an angular deformation of the NH_2 group δ (H–N–H). When compared to the value observed for the same conjugated frequency mode in the complex *cis*-[PtCl₂(PZA)₂], one can infer that the coordination to the platinum atom is in fact made via oxygen since the band is downshifted to 1677 cm^{-1} . On the other hand, the presence of two bands associated to modes ν (Pt–Cl), at 335 and 325 cm^{-1} , is an indicative of *cis* isomer. The calculated Gibbs energy (ΔG) of $16.8\text{ kcal mol}^{-1}$ points to the conformation represented by I in Figure 5a as the most stable in gas phase (-1905.834645 a.u. (I) vs. -1905.861408 a.u. (II)). The values confirm that the structure II is stabilized by the sum of electronic and free energy but destabilized by higher entropy by $0.34\text{ cal K}^{-1}\text{ mol}^{-1}$. This might be happened due to the formation of hydrogen bonds with the chlorine atoms (H–bond distance equal to 2.197 \AA), which does not occur in structure II. For this reason, structure I was chosen for further study.

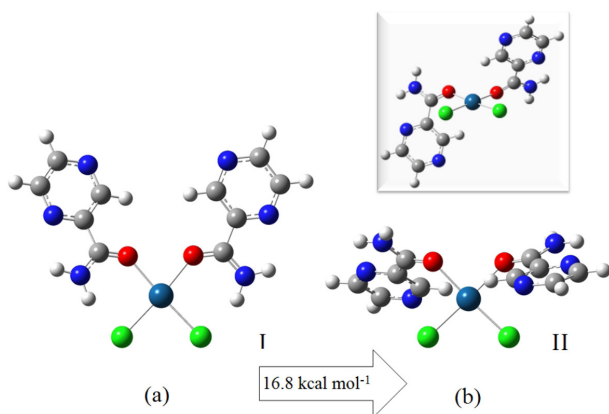


Figure 5. Energetic differences between two DFT optimized structures of *cis*-[PtCl₂(PZA)₂]. (a) Structure I, the most stable, and (b) structure II with two different views for clarification. Platinum is in the center of a square planar geometry. To check other labels, please refer to the chemical structure of Figure 2.

The comparative bond length and angle analyses for *cis*-[PtCl₂(PZA)₂] (I) and the free PZA ligand show the expected differences due to the metal center coordination. Moreover, the sizes of the new linkages present in the complex are in accordance to those that could be estimated from the proposed coordination mode. Both Pt–Cl bond distances are equal to 2.341 \AA and the Pt–O bond is equal to 2.116 \AA . The C=O bond lengths are equal to 1.252 \AA

for the complex and 1.221 \AA for the free PZA. This difference indicates a decreasing bond order, as expected from platinum coordination via the oxygen atom. The $\angle\text{Cl1–Pt–O1}$ angle (96.3°) is close to the $\angle\text{Cl2–Pt–O2}$ (97.2°), showing a distorted square planar geometry around the coordination sphere of platinum. This assignment can be confirmed with the dihedral involving the chlorine and oxygen atoms, which is of 1.23° . In addition, the dihedral Pt–O1–C1–C2 shows that the structure is almost entirely planar, with a slight deviation of only 2.5° between one PZA plane and the platinum coordination sphere.

The two proposed structures and those deviations shown around the dihedrals, labeled as D1: 4O/6C/11C/12N, D2: 2Cl/1Pt/5O/7C and D3: 1Pt/5O/7C/9C, led us to question structure I (Figure 5a) as the global minimum in potential energy surface. The literature shows some examples of different forms found after scan calculations or even after the intrinsic reaction calculation (IRC) from the transition state geometries.^{34,35} Because of this, rigid scan calculations was performed in order to uncover any other geometry with a lower energy value. These scans pointed to the same structure found for *cis*-[PtCl₂(PZA)₂] and this was decisive to search for another method which could indicate the better description and relationship of the geometry and energetic parameters.

Mixed-level factorial design

Factorial designs are very useful tools in obtaining deeper information about the relationships among the studied variables and to establish optimum experimental conditions. Their application to computational studies can be very interesting to reduce computational time and effort without losing quality of information. In the present case, a systematic approaching to the computational study of *cis*-[PtCl₂(PZA)₂], a 5×3 mixed-level factorial design taking into account the dihedral angle and dihedral factors was performed. Thus, a quantitative variable dihedral angle and a categorical variable dihedral were investigated at five and three levels, respectively (Table 2). This approach is very interesting since the optimum condition can be achieved by performing a small number of experiments.

The coefficients of the statistical model, using equation 1, were obtained as displayed in equation 2, containing percentage of explained variation, that is, R^2 equal to 0.945. Please, see the Supplementary Information to have access to the residual test and all Excel sheet.

$$y' = -1905.57 + 0.11X_1 - 0.68X_2 + 0.10X_1^2 + 0.60X_2^2 + 0.03X_1X_2 \quad (2)$$

(±0.11) (±0.07) (±0.06) (±0.12) (±0.11) (±0.09)

The significance effect was evaluated through a normal plot, as shown in Figure 6. The farther the points are from zero, the more significant the effects are. Thus, the main effect X_2 and the first order interaction X_2X_2 were considered significant within the investigated levels. In other words, the specific dihedral, in association with the dihedral angle, indicates the minimum energy.

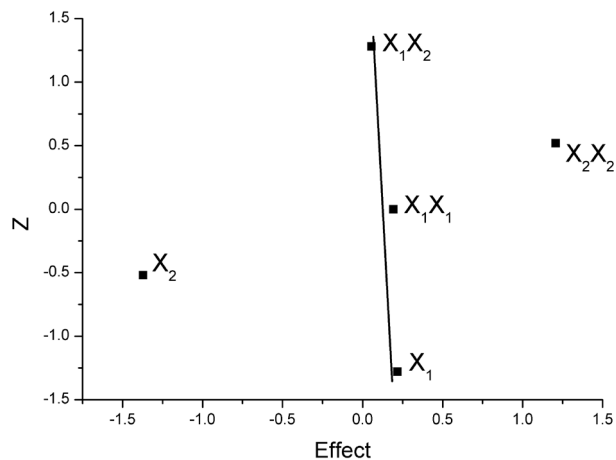


Figure 6. Normal plot showing the effects of the significances.

Thus, a response surface for the fitted model was investigated. However, before obtaining the response surface, it was necessary to verify the model lack of fit. In order to verify this, the Shapiro-Wilk normality test (the difference between observed and predicted values) was performed since it makes no sense to perform replicates to calculate experimental errors in theoretical work. In the present case, as the normality test resulted in a p -value of 0.215 ($p > 0.05$), the residues presented normal behavior within a 95% confidence interval. Thus, a response surface was obtained (Figure 7).

The response surface indicated that the minimum surface region of potential energy can be obtained when the dihedral angle is within an interval of $-0.8 \leq X_1 \leq -0.7$, fixing the dihedral in D2 (2Cl/1Pt/5O/7C). This is accurate since the minimum corresponds to the second derivative. Furthermore, seven additional experiments for validating the method (maintaining the D2 for dihedral angle fixed in 18.0°, 18.9°, 19.8°, 20.7°, 21.6°, 22.5° and 27°) were performed. The results indicate that the most stable

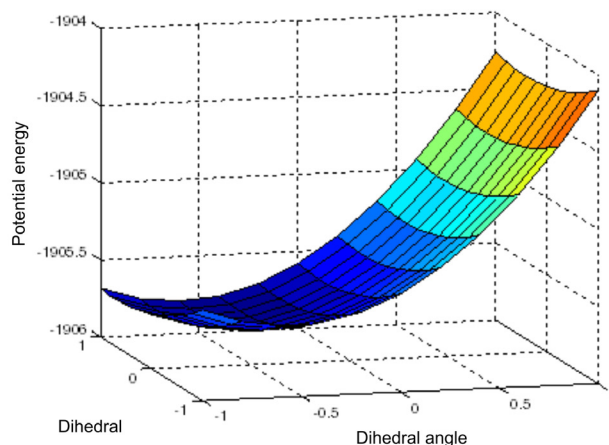


Figure 7. Response surface obtained for the 5×3 mixed experimental design.

conformation for the *cis*-[PtCl₂(PZA)₂] complex was verified for the dihedral two (D2) with an angle at 18.9°, according to Table 3. This table shows the correlations between the energies in atomic units and the validated values for dihedral D2. An optimization and frequency calculation considering the four D2 atoms freezing was performed in order to evaluate the energy and to compare to the values obtained through statistical methods. The result was quite remarkable precisely by 2.41 kcal mol⁻¹.

To the best of our knowledge, this work is the first to explore the combination of these two methods, molecular modeling and statistical techniques in order to help elucidate the geometry of a platinum(II) complex. Certainly, there are other articles that report the factorial design and principal component analysis studies associated to quantum chemical methods, like the one from De Azevedo *et al.*³⁶ applied to verify CH₃F infrared frequencies and intensities. However, the results showed here are interesting and put mixed-level factorial design at a new level if the method is well-applied. It is important to note that quantum mechanical methods, such as DFT, are very well established and there are no doubts about their reliability. However, in some cases, the search for the minimum point at the potential energy surface may indicate different structures. Therefore, the statistical technique used in the present study is consistent in verifying the most stable structure of the analyzed compound, with a relatively low computational effort.

Table 3. Results of the seven validation experiments for the dihedral D2

| | | | | |
|-------------------------|--------------|--------------|--------------|--------------|
| Dihedral angle / degree | 18.0 | 18.9 | 19.8 | 20.7 |
| Energy / a.u. | -1905.306587 | -1905.523093 | -1905.523079 | -1905.523059 |
| Dihedral angle / degree | 21.6 | 22.5 | 27.0 | |
| Energy / a.u. | -1905.523046 | -1905.523040 | -1904.585730 | |

Conclusions

To the best of our knowledge, the study of a platinum(II) complex with pyrazinamide (PZA) molecules as ligands is the first computational study associated to statistical methods. Since there are some possibilities for the best conformation, especially around three dihedral angles, a statistical analysis utilizing a mixed level factorial design was carried out, with the aim of correlating the stabilization energy and the best values for the dihedral angles.

Based on the behavior of the residues observed in the normal plot, the main effect X_1 and the interaction X_1X_2 were reliable in a 95% confidence interval. Thus, by the evaluation of the response surface and the implementation of seven experiments to validate the region identified as optimal, we inferred that the most stable geometry, i.e., with the lowest potential energy, refers to the dihedral $2Cl_1Pt/5O/7C$ with an angle of 18.9° . Therefore, the use of a mixed level factorial design associated to a computational study allowed to optimize system stability, evaluate interaction effects and diminish computational effort since only 22 experiments were necessary: 15 factorial and 7 to validate the area indicated as optimal.

Further studies involving the full chemical characterization of $[PtCl_2(PZA)_2]$, as well as its performance as an anticancer agent towards human tumoral cells, are underway and will be the subject of future reports.

Supplementary Information

Excel sheet including coefficient errors and graphic of residues is available free of charge at <http://jbcs.sbq.org.br> as a PDF file.

Acknowledgements

P. A. S. Oliveira thanks the scholarship received during her time at NEQC (PROBIC-FAPEMIG); N. A. R. is grateful to CNPq for the research fellowship awarded; H. F. Dos Santos thanks FAPEMIG and CNPq; M. A. L. De Oliveira wishes to acknowledge CNPq (475055/2011-0 and 301689/2011-3) and FAPEMIG (CEX-APQ-02420-11 and CEX-PPM 00205-11). L. A. S. Costa is grateful to FAPEMIG for the funds received from the award project (CEX-APQ-02967-10).

References

- Zhang, J. Z.; Bryce, N. S.; Lanzirrotti, A.; Chen, C. K. J.; Paterson, D.; de Jonge, M. D.; Howard, D. L.; Hambley, T. W.; *Metallomics* **2012**, *4*, 1209.

- Matos, C. S.; de Carvalho, A. L. M. B.; Lopes, R. P.; Marques, M. P. M.; *Curr. Topics Med. Chem.* **2012**, *19*, 4678.
- Rosenberg, B.; Van Camp, L.; Krigas, T.; *Nature* **1965**, *205*, 698.
- Rosenberg, B.; Van Camp, L.; Trosko, J. E.; Mansour, V. H.; *Nature* **1969**, *222*, 385.
- Kelland, L. R.; *Nat. Rev. Cancer* **2007**, *7*, 573.
- Reedijk, J.; *Pure Appl. Chem.* **2011**, *83*, 1709.
- Komeda, S.; Casini, A.; *Curr. Topics Med. Chem.* **2012**, *12*, 219.
- Liu, H.-K.; Sadler, P. J.; *Accounts of Chemical Research* **2011**, *44*, 349.
- Ang, W. H.; Myint, M.; Lippard, S. J.; *J. Am. Chem. Soc.* **2010**, *132*, 7429.
- Benedetti, B. T.; Quintal, S.; Farrell, N. P.; *Dalton Trans.* **2011**, *40*, 10983.
- Hall, M. D.; Daly, H. L.; Zhang, J. Z.; Zhang, M.; Alderden, R. A.; Pursche, D.; Foranc, G. J.; Hambley, T. W.; *Metallomics* **2012**, *4*, 568.
- Blanchard, J. S.; *Ann. Rev. Biochem.* **1996**, *65*, 215.
- Akyuz, S.; *J. Mol. Struct.* **2003**, *541*, 651.
- Shi, R.; Itagaki, N.; Sugawara, I.; *Mini Rev. Med. Chem.* **2007**, *7*, 1177.
- Akalin, E.; Akyuz, S.; *J. Mol. Struct.* **2007**, *834–836*, 492.
- Chiş, V.; Pîrnău, A.; Jurcă, T.; Vasilescu, M.; Simon, S.; Cozar, O.; David, L.; *Chem. Phys.* **2005**, *316*, 153.
- Hazarika, K. K.; Baruah, N. C.; Deka, R. C.; *Struct. Chem.* **2009**, *20*, 1079.
- Bischin, C.; Lupan, A.; Taciuc, V.; Silaghi-Dumitrescu, R.; *Mini Rev. Med. Chem.* **2011**, *11*, 214.
- Guddneppanavar, R.; Saluta, G.; Kucera, G. L.; Bierbach, U.; *J. Med. Chem.* **2006**, *46*, 3204.
- Polonini, H. C.; de Oliveira, M. A. L.; Ferreira, A. O.; Raposo, N. R. B.; Grossic, L. N.; Brandão, M. A. F.; *J. Braz. Chem. Soc.* **2011**, *22*, 1263.
- Becke, A. D.; *J. Chem. Phys.* **1993**, *98*, 5648.
- Lee, C.; Yang, W.; Parr, R. G.; *Phys. Rev. B* **1988**, *37*, 785.
- Ditchfield, R.; Hehre, W. J.; Pople, J. A.; *J. Chem. Phys.* **1971**, *54*, 724.
- Hehre, W. J.; Ditchfield, R.; Pople, J. A.; *J. Chem. Phys.* **1972**, *56*, 2257.
- Hay, P. J.; Wadt, W. R.; *J. Chem. Phys.* **1985**, *82*, 270.
- Wadt, W. R.; Hay, P. J.; *J. Chem. Phys.* **1985**, *82*, 284.
- Hay, P. J.; Wadt, W. R.; *J. Chem. Phys.* **1985**, *82*, 299.
- Costa, L. A. S.; Hambley, T. W.; Rocha, W. R.; De Almeida, W. B.; Dos Santos, H. F.; *Intl. J. Quant. Chem.* **2006**, *106*, 2129.
- Da Silva, V. J.; Costa, L. A. S.; Dos Santos, H. F.; *Intl. J. Quant. Chem.* **2008**, *108*, 401.
- Foresman, J. B.; Frisch, A.; *Exploring Chemistry with Electronic Structural Methods*, 2nd ed.; Gaussian, Inc.: Pittsburgh, 1996.
- Gaussian 09, Revision A.02*, Frisch, M. J.; Trucks, G. W.; Schlegel, H. B.; Scuseria, G. E.; Robb, M. A.; Cheeseman,

- J. R.; Scalmani, G.; Barone, V.; Mennucci, B.; Petersson, G. A.; Nakatsuji, H.; Caricato, M.; Li, X.; Hratchian, H. P.; Izmaylov, A. F.; Bloino, J.; Zheng, G.; Sonnenberg, J. L.; Hada, M.; Ehara, M.; Toyota, K.; Fukuda, R.; Hasegawa, J.; Ishida, M.; Nakajima, T.; Honda, Y.; Kitao, O.; Nakai, H.; Vreven, T.; Montgomery, Jr., J. A.; Peralta, J. E.; Ogliaro, F.; Bearpark, M.; Heyd, J. J.; Brothers, E.; Kudin, K. N.; Staroverov, V. N.; Kobayashi, R.; Normand, J.; Raghavachari, K.; Rendell, A.; Burant, J. C.; Iyengar, S. S.; Tomasi, J.; Cossi, M.; Rega, N.; Millam, J. M.; Klene, M.; Knox, J. E.; Cross, J. B.; Bakken, V.; Adamo, C.; Jaramillo, J.; Gomperts, R.; Stratmann, R. E.; Yazyev, O.; Austin, A. J.; Cammi, R.; Pomelli, C.; Ochterski, J. W.; Martin, R. L.; Morokuma, K.; Zakrzewski, V. G.; Voth, G. A.; Salvador, P.; Dannenberg, J. J.; Dapprich, S.; Daniels, A. D.; Farkas, Ö.; Foresman, J. B.; Ortiz, J. V.; Cioslowski, J.; Fox, D. J. Gaussian Inc., Wallingford CT, 2009.
32. Montgomery, D. C.; *Design and Analysis of Experiments*, 6th ed.; Wiley: New York, USA, 2004.
33. Barros Neto, B.; Scarminio, I. S.; Bruns, R. E.; *Como fazer Experimentos: Pesquisa e Desenvolvimento na Ciência e na Indústria*, 4^a ed.; Bookman: Porto Alegre, Brasil, 2010.
34. Hratchian, H. P.; Schlegel, H. B.; *Theory and Applications of Computational Chemistry: The First 40 Years*; Dykstra, C. E.; Frenking, G.; Kim, K. S.; Scuseria, G., eds.; Elsevier: Amsterdam, The Netherlands, 2005.
35. Costa, L. A. S.; T. W.; Rocha, W. R.; De Almeida, W. B.; Dos Santos, H. F.; *Chem. Phys. Lett.* **2004**, *387*, 182.
36. De Azevedo, A. L. M. S.; Barros Neto, B.; Scarminio, I. S.; De Oliveira, A. E.; Bruns, R. E.; *J. Comp. Chem.* **1996**, *17*, 167.

Submitted: May 25, 2013

Published online: September 4, 2013